Human Brain (2022) 1(1), 3–20
https://doi.org/10.37819/hb.001.001.0206

eurasia

ORIGINAL RESEACH ARTICLE

Check for updates

Characterization of a new set of monoclonal β-amyloid antibodies

Huan-Yu Che[1#*], Jia-Qi Ai[2#], Chen Yang[2], Xiao-Lu Cai[2], Yan Wang[2], Juan Jiang[2], Qi-Lei Zhang[2], Tian Tu[3], Ewen Tu[4], Chong Che[5], Xiao-Xin Yan[2*]

[1]*School of Medical Pharmacy, Tonghua Normal University, Tonghua, Jilin 134002, China*
[2]*Department of Anatomy and Neurobiology, Central South University Xiangya School of Medicine, Changsha, Hunan 410013, China*
[3]*Department of Neurology, Xiangya Hospital, Changsha, Hunan 410008, China*
[4]*Department of Neurology, Brain Hospital of Hunan Province, Changsha, Hunan 410007, China*
[5]*GeneScience Pharmaceuticals Co., Ltd., Changchun High-Tech Development Zone, Changchun, Jilin 130012, China*
[#]*Authors contributed equally to the current study*

**Correspondence should be addressed to: Email addresses: Huan-Yu Che: chehuanyu0119@163.com; Jia-Qi Ai: aijiaqi9523@163.com; Chen Yang: 1504046898@qq.com; Xiao-Lu Cai: 2433308289@qq.com; Yan Wang: wy17873678578@163.com; Juan Jiang: 838525203@qq.com; Qi-Lei Zhang: zhangqilei1011@icloud.com; Tian Tu: tutian1991@163.com; Ewen Tu: tuewen612@163.com; Chong Che: chechong@gensci-china.com; Xiao-Xin Yan: yanxiaoxin@csu.edu.cn*

ABSTRACT

β-Amyloid (Aβ) deposition is a commonly studied neuropathology in the human brain, occurring as compact and diffuse parenchymal plaques, cerebral amyloid angiopathy (CAA), and meningeal/subpial amyloidosis. Compact plaques associated with dystrophic neurites generally referred to as neuritic plaques, are a pathological hallmark of Alzheimer's disease (AD). We evaluated three recently developed monoclonal mouse antibodies against Aβ (A1, A2 and A3) using appropriate tissue samples and assay controls in the present study. In immunohistochemistry, antibodies A1, A2 and A3 displayed all forms of cerebral Aβ deposition in a range of dilutions in cryostat and paraffin sections. These labeled profiles appeared morphologically comparable to that visualized by two commercial Aβ antibody clones, 6E10 and D12B2. In immune-dot blotting assays, antibodies A1, A2 and A3 at highly diluted concentrations detected an increase of Aβ in neocortical lysates of AD samples compared to control. Moreover, these antibodies clearly labeled Aβ pathology in brain sections of three commonly used transgenic mouse models of AD, namely, APP/PS1 mice, 5XFAD mice, and 3XTg-AD mice. Taken together, these monoclonal mouse anti-Aβ antibodies can serve as new experimental tools for basic, translational, and diagnostic research into aging and AD-related cerebral Aβ neuropathology in both human and experimental animal brains.

ARTICLE HISTORY

Received: 17-04-2022
Revised: 13-07-2022
Accepted: 9-09-2022

KEYWORDS

Brain aging;
Dementia;
Neurodegeneration;
Neuritic plaque;
Proteostasis;
Vps10p

Introduction

β-Amyloid peptides (Aβ) are produced from the proteolytic cleavage of β-amyloid precursor protein (APP) by β-secretase 1 (BACE1) and ɤ-secretase (Yan et al., 2007; Checler et al., 2021; Hampel et al., 2021; Cho et al., 2022; Hur, 2022; Patel et al., 2022). The Aβ products were first discovered by biochemical identification using isolated human brain samples of the cerebral amyloid vasculature and parenchymal plaques (Glenner and Wong, 1984; Masters et al., 1985). This characterization, along with the identification of phosphorylated tau (pTau) as a component of neurofibrillary tangles (Grundke-Iqbal, 1986; Wischik et al., 1988; Goedert et al., 1988; Novak et al., 1989; Alonso Adel et al., 2013), marked the most influential milestone in the history of research into Alzheimer's disease (AD) (Beach, 2022). Since these fundamental discoveries in the mid-1980s, numerous Aβ and pTau antibodies have been developed, serving as essential histological tools for pathological diagnosis, pathogenic investigation, and basic and translational research in AD (Braak and Braak, 1991; Thal et al., 2002; Braak and Del Tredici, 2014; Serrano-Pozo et al., 2011; Khurshid et al., 2022). During the past two decades, Aβ and pTau antibodies have been increasingly explored as biofluid detecting reagents for risk assessment of AD and other dementia disorders among living elderly patients (Guzman-Martinez et al., 2019; Alawode et al., 2021; Park et al., 2022). Significantly, pharmaceutical companies have developed several humanized monoclonal Aβ and pTau antibodies tested as potential mechanism-based therapeutics for the prevention and treatment of AD (Caselli et al., 2017; Jeremic et al., 2021). Therefore, Aβ and pTau antibody development remain active in current mechanistic and translational research in the AD field.

Historically, most neuropathological research into human brain diseases, including AD, has been overwhelmingly performed by institutions in Western countries (Critchley, 1929; Oĭfa, 1973; García-Marín et al., 2007; Ohry et al., 2015). There is very little in the literature on the neuropathological characterization of human brain diseases in the brains of Chinese subjects, given that China has the world's most outstanding and most significant population (Tang et al., 2020). However, there has been substantial progress in human brain banking in China (Yan et al., 2015; Xu et al., 2016; Ma et al., 2019). Postmortem brains preserved by several major institutions in China have recently become an essential resource in support of neuropathological and explorative studies by Chinese investigators of AD (Hu et al., 2017; Zhou et al., 2018; Xiong., 2019; Zhang et al., 2019; Zhu et al., 2019; Zhang et al., 2020; Shi et al., 2020; Tu et al., 2020; Cong et al., 2021; Jia et al., 2021; Liu et al., 2021; Jiang et al., 2022; Gao et al., 2022; Yang et al., 2022). Part of the standard operational protocol of brain banking involves the evaluation of AD-related pathologies (Qiu et al., 2019). Therefore, reliable and financially affordable antibodies can potentially support the examination of Aβ and pTau pathologies in human brain samples, especially in the Chinese population, which would provide basic comparisons with AD research from Western countries.

In the present study, we conducted histological and biochemical evaluations on 3 recently developed monoclonal mouse antibodies against Aβ, A1, A2 and A3, using post-mortem human brain samples. The specificity and potency of these antibodies in detecting Aβ change were determined in immunohistochemical, immuno-dot and Western blot assays using positive and negative pathological controls. Well-established commercial antibodies were used as assay control tools and compared with these new antibodies.

Materials and methods

Brain samples and tissue preparation

The Ethics Committee approved the current study of Central South University Xiangya School of Medicine, following the Code of Ethics of the World Medical Association (Declaration of Helsinki). Brains were collected post-mortem through a willed body donation program with antemortem consent by the Donor or the next-of-kin (Yan et al., 2015). Donor's clinical records before and/or during the last hospitalization were obtained whenever available. Brain preparation and histopathological evaluation were carried out according to the Standard Brain Banking Protocol set by China Brain Bank Consortium (Qiu et al., 2019). Following removal from the skull, the brain was bisected, with one half (right-side or the non-hand-dominant side) fresh-frozen at -70 °C

(for future biochemical studies) and the other half (left-side or the hand-dominant side) immersed in formalin (10% formaldehyde) for 2-4 weeks. The fixed hemi-brain was then cut coronally into 10 mm thick slices and further preserved in a diluted formalin solution (5% formaldehyde) with sucrose (15%) at 4 °C. Tissue blocks were dissected from the fixed slices for the preparations of both cryostat and paraffin sections. Forty-micron thickness consecutive cryostat sections were cut and stored in a cryoprotectant solution (30% sucrose, 1% polyvinyl-pyrrolidone and 30% ethylene glycol in 0.1 M phosphate buffer) at -20 °C before use. Furthermore, eight-micron paraffin sections were cut from the tissue blocks.

For this study, frozen and paraffin sections of formalin-fixed samples from four aged cases with late-stage AD-like neuropathology, and four control cases free of neuropathology, were used for histopathological evaluation of the new Aβ antibodies. For immune-dot and Western blotting experiments, samples were chipped from the frozen frontal cortical slices at the lateral orbital gyrus. The case information and neuropathological staging of the brains are provided in Table 1. In addition to the human brain samples, cryoprotected sections of perfused brains from three lines of transgenic mouse models, namely the APP/PS1, 5XFAD and 3XTg-AD mice, were used in the present study. The neuropathological evaluations of these animal brain tissues were reported in previous studies (Zhang et al., 2009; Cai et al., 2012; Griffith et al., 2016; Macklin et al., 2016; Zhou et al., 2018).

Antibodies

The new monoclonal Aβ antibodies were the secretion products of a selected batch of cultured hybridoma lines obtained from mice immunized with synthetic Aβ42 peptide, following established protocol for the generation and screening of monoclonal antibodies (Li et al., 2010). After initial immunohistochemical assessments, the supernatants from three separate clones of hybridoma lines, A1, A2 and A3, were identified and subjected to a thorough characterization in this study. The details of antibody production and initial evaluation were described elsewhere (patents #CN111518206A, CN111518206B and CN111518205B). Purified A1, A2 and A3 antibodies were supplied as stock solutions at concentrations of 2.43 mg/ml, 7.14 mg/ml and 2.24 mg/ml, respectively, in 20 mM sodium citrate and 30mM Tris buffer (pH 7.0). For the use in immunohistochemical, immune-dot and immunoblot experiments, the antibodies were then titred to various concentrations ranging from high to low. Two commercial Aβ antibodies were used in the experiments for assay/quality control, including the mouse anti-Aβ antibody clone 6E10 (Cat#39320, Signet Laboratories, Inc., Dedham, MA, USA) and rabbit monoclonal anti-Aβ antibody clone D12B2 (Cat#9888, Cell Signaling Technology, Danvers, MA, USA). In addition, the mouse monoclonal anti-pTau antibody clone AT8 (Cat#MN1020B, ThermoFisher Scientific, Waltham, MA, USA) was used to confirm intraneuronal accumulation of hyper-phosphorylated tau in the sections of AD brains.

	Case #	Age (y)	Sex	Clinical diagnosis and cause of death	Post-mortem delay (h)	Braak NFT stage	Thal Aβ phase
Negative control cases without AD pathology (n=4; 84.3±5.0)	1	79	M	Stroke	2	0	0
	2	89	F	Multisystem failure	16	0	0
	3	81	M	Cardiovascular failure	6	0	0
	4	88	F	Coronary heart disease	9	0	0
Positive control cases with AD pathology (n=4; 90.9±11.0)	5	74	F	Lung cancer (small cell)	5	IV	4
	6	98	M	Multiple system failure*	7	IV	4
	7	96	M	Heart Disease*	20	VI	5
	8	92	M	Coronary heart disease*	12	VI	5

*Demented according to the last clinical report or enquiry with the next-of-kin of the Donor. Braak neurofibrillary tangle (NFT) stages were assessed according to immunolabeling with the AT8 antibody to phosphorylated tau (pTau). Thal β-amyloid (Aβ) phases were evaluated according to immunolabeling with the 6E10 antibody against the N-terminal sequence (amino acid residues 1-16) of Aβ.

Table 1. Demographic information of brain donors and staging of Alzheimer-related neuropathology

Immunohistochemistry

Multiple sets of consecutive cryostat or paraffin sections from the temporal and frontal lobes were processed in parallel immunohistochemistry using an avidin-biotin complex (ABC)-peroxidase method according to a previously established protocol (Hu et al., 2017; Tu et al., 2020). Each antibody's sections from the positive and negative AD pathological cases were stained under identical conditions. Individual sections were stained with the A1, A2 and A3 antibodies using a series of concentrations (1:100 and above). An additional set of sections were also stained with the 6E10 (diluted at 1 to 1000), D12B2 (1:2000) or AT8 (1:2000) antibodies at an optimized dilution, respectively, as assay controls. Following incubation with the primary antibody in 0.01 M phosphate-buffered saline (PBS), sections were then incubated with a pan-specific secondary antibody, i.e., biotinylated horse anti-mouse, rabbit and goat IgGs (1:400; Vector Labs., Burlingame, CA, United States), then the ABC reagents (1:400; Vector Labs., Burlingame, CA, United States). The immunoreaction product was visualized with a solution containing peroxidase (0.003%) and diaminobenzidine (DAB, 0.05%). The washes in PBS for 10 min were carried out between the incubations. In addition, some sections were counterstained with hematoxylin for neuroanatomical orientation as needed. Finally, the sections were dehydrated with ascending ethanol solutions, cleared with xylene, and coverslipped with the Permount™ mounting medium (Electron Microscopy Science, USA).

Immuno-dot blot

Neocortical samples obtained from frozen frontal neocortices of 3 control (#1, 3, 4 in Table 1) and 3 AD (#5, #6 and #8) cases were homogenized on ice by sonication in RIPA extraction buffer (ThermoFisher, #J62524.AE, diluted to 1X concentration). Extracts were centrifuged at 15,000 g at 4◦C, and the supernatants were collected. This was followed by a DC protein assay (Bio-Rad Laboratories, Hercules, CA, USA) to determine the protein concentrations. For the immune-dot assay, lysates containing an equal amount of total protein (10 µl) were directly dropped on nitrocellulose membranes in rows. The membranes were allowed to air dry for 24 hrs and then cut into strips so each strip contained one dot-load of samples from each positive and negative AD pathological case. Afterwards, the strips were immunochemically stained with the mouse anti-Aβ A1, A2, and A3 at tittered concentrations (3 times dilution started from 1:100), respectively. The immunoreaction product on the membrane was visualized by incubations sequentially with biotinylated horse anti-mouse IgG (1:400) and ABC complex (1:400), respectively, and finally with a solution containing peroxidase (0.003%) and diaminobenzidine (DAB, 0.05%).

Western blot

Cortical supernatants prepared as above were run with sodium dodecyl sulfate-polyacrylamide gel electrophoresis (SDS-PAGE, 10% or 15%). Separated protein products were electrotransferred to Trans-Blot pure nitrocellulose membranes. Membrane strips were incubated with the A1, A2 and A3 antibodies (diluted at 1:300, 1:900, 1:2700 and 1:8100, respectively) as well as the commercial antibodies 6E10 (1:300, 1:900) and D12B2 (1:300, 1:900, 1:2700 and 1:8100). The strips were further incubated with HRP-conjugated goat anti-mouse or anti-rabbit secondary antibodies (1:10,000; Bio-Rad Laboratories, Hercules, CA, USA), with the signal developed using the ECL-plus Western blotting substrate detection kit (ThermoFisher Scientific; Waltham, MA, USA). After image capture of the above blotting products, the membranes were washed in a stripping buffer (Abcam, Cat#ab282569), followed by reblotting of glyceraldehyde-3-phosphate dehydrogenase (GAPDH) (mouse antibody, 1:5000, Millipore Shanghai Trading Company Ltd., Shanghai, China) to determine the levels of the internal protein loading control.

Image acquisition, data analysis and figure preparation

Immunolabeled sections were scan-imaged using the 40× objective on a Motic-Olympus microscope equipped with an automated stage and imaging system (Motic China Group Co. Ltd., Wuhan, Hubei, China). The images were examined with the Motic viewer (Motic Digital Slide Assistant System Lite 1.0, Motic China Group Co. Ltd.) to assess the labeling across low- to high-resolution anatomical regions. Images covering the whole tissue section and anatomical areas of interest were extracted at desired magnifications and

exported for figure preparation. The pictures of the immune-dot were captured with a high-resolution digital camera and saved as digital documents. Western blot images were documented with the UVP ChemStudio/PLUS device (Analytik-Jena/UVP, USA).

Quantitative image analysis (densitometry) was performed for the immune-dot data using the OptiQuant software (Packard Instruments, Meriden, CT, USA). The circular selection tool was used to measure the optical densities (o.d.) over the blotted dots. The background o.d. was obtained over an area outside the sample loading spots using the rectangular selection tool. The density data were then exported into Excel spreadsheets, with the specific o.d. calculated by subtracting the background o.d. from the o.d. over the sample loading dots. The antibody concentrations converted into log scales (log[mg/ml], were calculated according to the diluted titers and the original concentration of the stock solution. The processed data were then entered into Prism spreadsheets and graphed (Prism GraphPad, San Diego, CA, USA). Statistical analysis was carried out with a student-t-test (one-tail paired), with $P<0.05$ as the cutting level for a significant difference. Figures were assembled with Photoshop 8.0.

Results

Antibodies A1, A2 and A3 detected Aβ pathology

As a part of positive assay and sample controls, we used two commercial Aβ antibodies, 6E10 and D12B2, and the monoclonal pTau antibody AT8 to verify the presence of these two lesions in sections of the selected cases with and without AD neuropathology. In identically processed paraffin or cryostat (data not shown) frontal and temporal lobe sections, 6E10 and D12B2 selectively detected extracellular Aβ deposits in the sections from the cases with AD pathology, whereas no deposition was seen in the pathologically negative control (Fig. 1A, B). At high magnifications, the labeled Aβ deposits were microscopically characteristic of compact parenchymal plaques, diffuse plaques, and CAA (see arrow), as well as meningeal and subpial amyloidosis (Fig. 1A1, B1). The pTau antibody AT8 labeled intraneuronal hyper-phosphorylated tau in a subpopulation of cortical and hippocampal neurons in the somata and neuritic processes paraffin (Fig. 1C, C1) and cryostat (Fig. 1D, D1) sections from the cases with AD pathology. In contrast, no specific immunolabeling occurred in the pathologically negative control. At higher magnifications, pTau positive neurons showed variable labeling intensity, with the heavily labeled ones appearing to be filled with tangles (Fig. 1C2, C3, D2, D3, examples pointed by arrows). pTau immunoreactive neuronal processes were present in the neocortex's gray and white matter areas and hippocampal formation. Some pTau-labeled processes appeared to be plaque-associated dystrophic neurites, given that they were arranged in clusters (Fig. 1C3, D3, pointed by arrowheads).

In a set of paraffin sections containing sections verified (as above) to be positive and negative with AD pathology, the antibody A1 labeled Aβ deposition in the AD but not control sections at all dilutions from 1:100 up to 1:24300 of the original concentration (2.43 mg/ml) (Fig. 2). At high magnifications, the labeled Aβ pathology was seen as compact and diffuse plaques, CAA and meningeal amyloidosis microscopically (Fig. 2A3, B3, C3, D3, E3, F3). Typical compact plaques were easily recognized (Fig. 2F3, see arrow). There was a relatively higher background labeling in the cases with low (Fig. 2A, B) compared to high (Fig. 2C, D, E, F) antibody dilutions. Shown as an example, at 1:10000 dilution, this antibody also selectively visualized Aβ deposition in the cryostat neocortical section from an AD case. In contrast, no labeling was present in the identically processed section from a control case (Fig. 2G, G1).

In a set of frozen frontal cortical sections from an AD case processed in parallel in the same experiment, the antibody A2 labeled Aβ deposits at a dilution from 1:300 up to 1:72900 of the original stock concentration (7.14mg/ml) (Fig. 3). The plaques were not microscopically distinct because of a high background reactivity in the low dilution groups (1:300 to 1:2700) (Fig. 3A-A2, B-B2, and C-C2). In contrast, high antibody dilutions yielded more distinctly immunolabeled plaques as the background reactivity was reduced (Fig. 3D-D2, E-E2, and F-F2). At 1:36000 dilution, antibody A2 clearly labelled Aβ plaques and CAA in the paraffin neocortical section from an AD case, whereas no staining was observed in the section from a control case (Fig. 3G, G1 and G2).

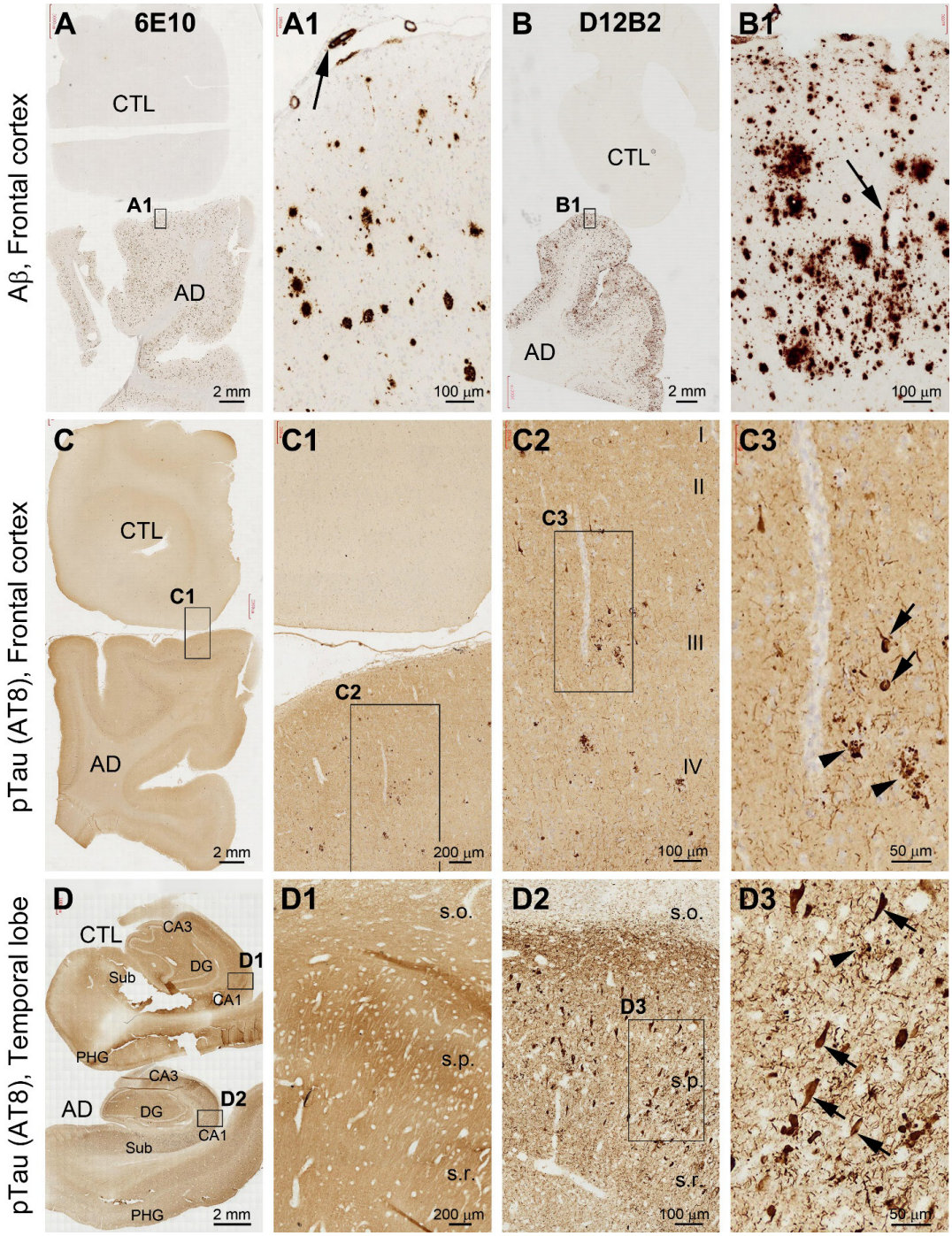

Figure 1. Immunolabeling of β-amyloid and tau pathology with positive control antibodies in sections from cases with and without AD-type neuropathology. Case information, antibodies, image orientation and scale bars are as indicated. The 6E10 and D12B2 antibodies selectively label Aβ in sections from AD but not in control (CTL) cases **(A, A1; B, B1)**. This was also the case for AT8 antibody labeling of intraneuronal tau accumulation **(C-C3, D-D3)**. Panels A-C3 are images from paraffin sections, and **(D-D3)** from cryostat sections. Arrows point to cerebral amyloid angiopathy (CAA), to tangle-filled neurons in C3 and D3. Arrowheads point to dystrophic neurites in C3 and D3. Additional abbreviations: CA1, CA2, and CA3: Ammon's horn sectors; DG: dentate gyrus; Sub: subiculum; PHG: parahippocampal gyrus; s.o. stratum oriens; s.p.: stratum pyramidale; s.r.: stratum radiatum. I-VI: cortical layers.

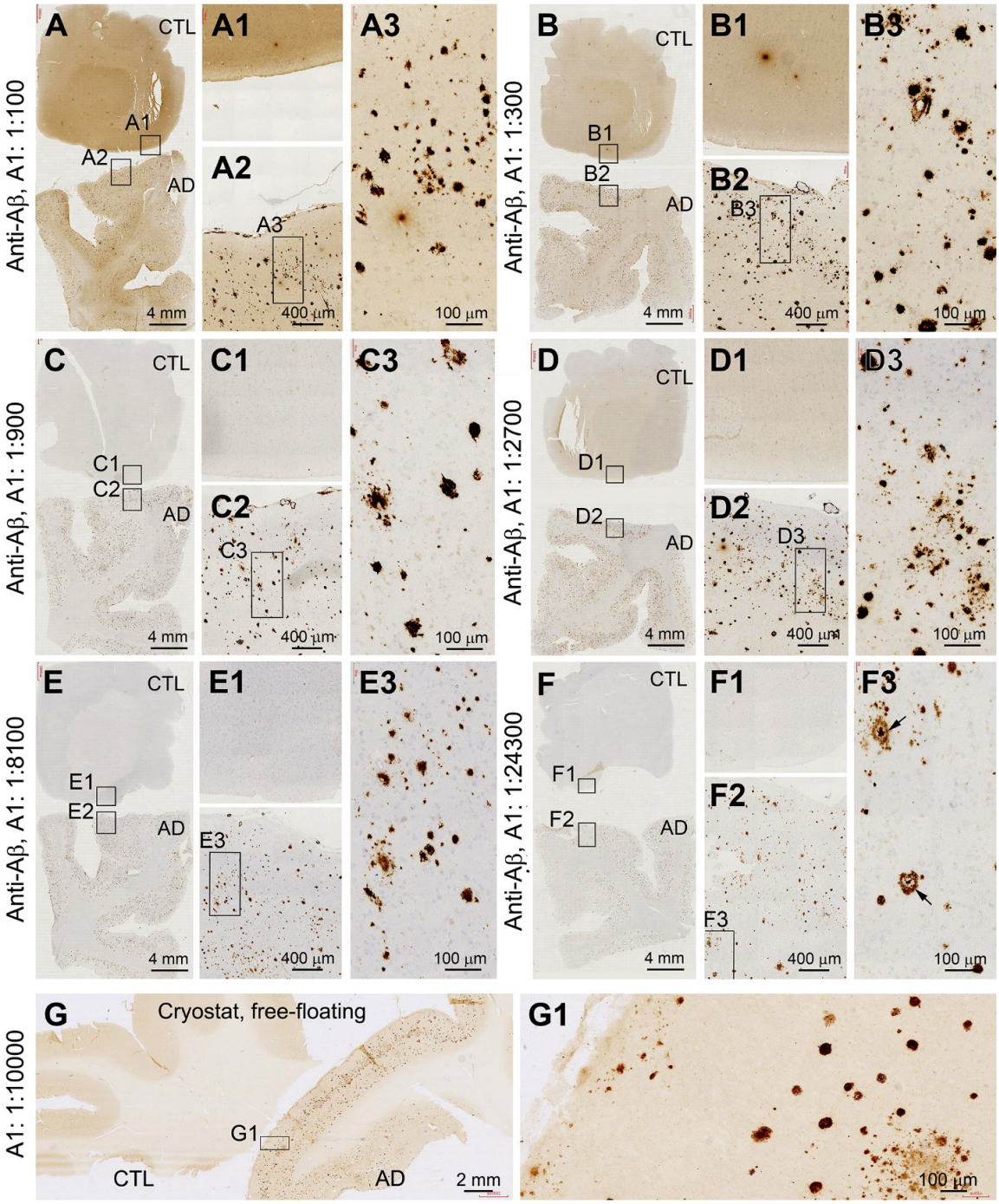

Figure 2. Immunolabeling of monoclonal antibody A1 in paraffin and cryostat sections from cases with and without AD-type neuropathology. Case information, antibody dilution, image orientation and scale bars are as indicated. The A1 antibody at a range of dilutions selectively labels Aβ in paraffin sections from AD but not control (CTL) cases **(A-F1)**. It also labels Aβ pathology in the cryostat section from an AD but not in the control cases **(G-G1)**. Arrows in F3 show coned compact plaques.

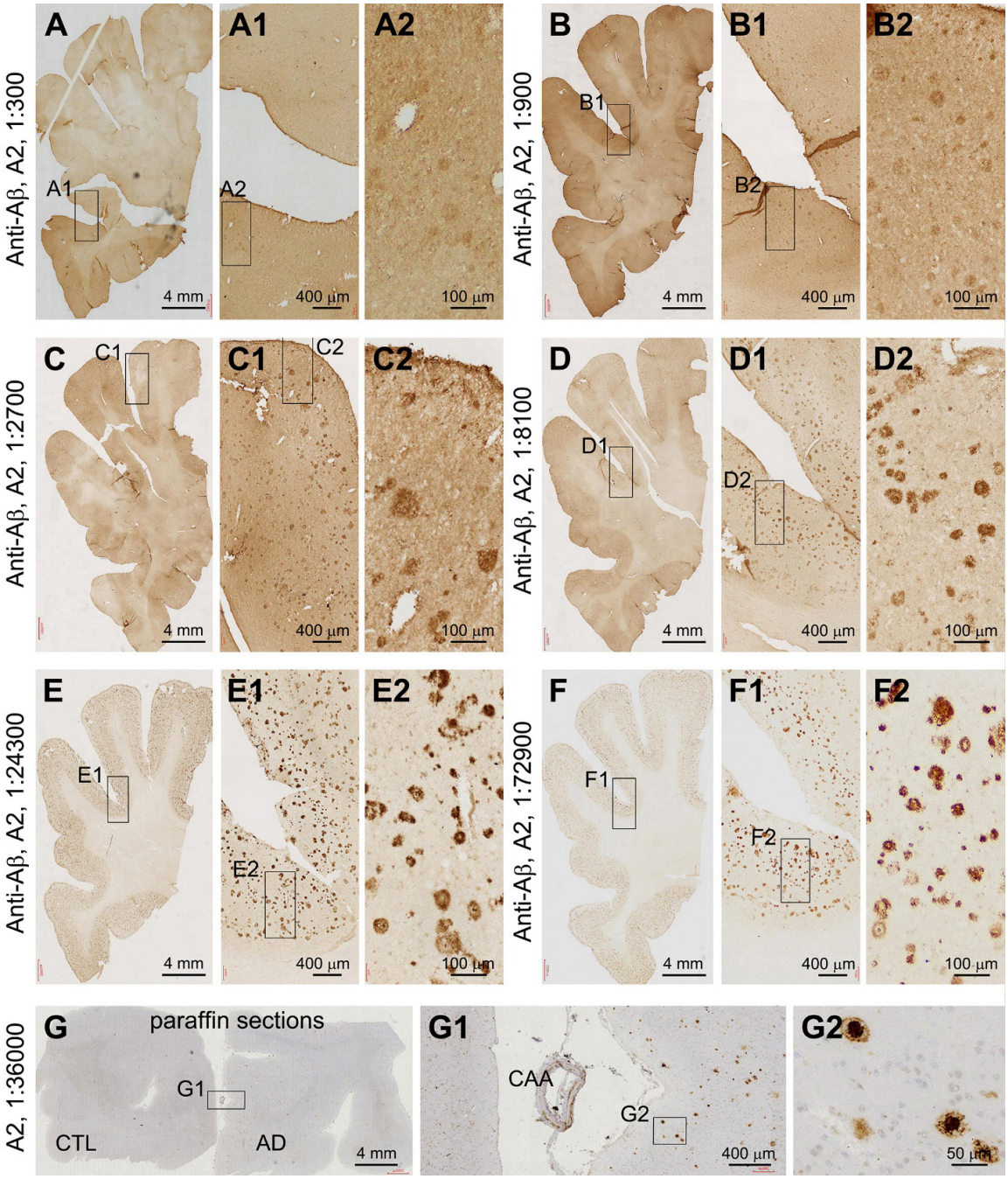

Figure 3. Immunolabeling of monoclonal antibody A2 in cryostat and paraffin sections from cases with and without AD-type neuropathology. Case information, antibody dilution, image orientation and scale bars are as indicated. The A2 antibody selectively labels Aβ in frozen sections from an AD case **(A-F2)** at various dilutions. A2 also labels Aβ in paraffin sections from an AD case but not in control cases (G-G1) at a dilution of 1:36000 **(G, G1)**. Cerebral amyloid angiopathy (CAA) and cored compact plaques can be clearly observed in some high magnification panels **(E2, F2, G1 and G2)**.

As illustrated with a set of images of immunolabeled cryostat frontal cortical sections from an AD case (Fig. 4A-F2), antibody A3 could detect Aβ deposition at a range of working dilutions from the original stock concentration (2.24 mg/ml). No Aβ deposition was observed in parallelly prepared cortical sections from control cases (data not shown). As with the case of antibodies A1 and A2 aforementioned, high background reactivity was seen in the sections processed with the A3 antibody at lower dilutions (1:100 to 1:900) (Fig. 4A-A2, B-B2, C-C2 and D-D2). Thus, the plaques appeared more microscopically distinct in the sections immunolabeled with A3 diluted at 1:2700 (Fig. 4D-D2) and 1:8100 (Fig. 4E-E2) because of the decline of the background reactivity. However, the specific plaque labeling became less intense and precise in the sections stained with the antibody diluted at 1:24300 (Fig. 4F-F2). It should be noted that this antibody could not effectively visualized Aβ deposition in paraffin sections (Fig. 4G and G1). However, we used various dilutions and several antigen retrieval methods (data not shown).

Antibodies A1, A2, and A3 detected Aβ elevation in immune-dot assay

We next carried out immune-dot blotting assays to evaluate the utility and potency of the monoclonal antibodies in detecting Aβ levels in brain lysates, using extracts from three AD pathology positive and three negative cases with relatively shorter post-mortem delays (Table 1). Exact amounts of total protein (10 μl) of the extracts were drop-loaded onto nitrocellulose membranes, followed by incubation with A1, A2 and A3 at different dilutions and immunoreactivity was visualized (Fig. 5A, B). The blotted signal was higher in all the AD pathology positive samples than in the negative control cases, with an antibody concentration-dependent effect seen in the dots from each AD pathology positive case. Based on the densitometric analysis, the difference in the mean optic densities between the AD pathology positive and negative cases was generally more significant in the conditions where the antibodies were diluted to relatively low concentrations, i.e., 1:900 and more (Fig. 4C-E). Thus, antibodies A1, A2 and A3 detected significantly elevated Aβ levels in the cases relative to those without microscopically verified AD pathology, with their dilutions as low as log -4 [mg/ml] for all of the three monoclonal antibodies (Fig. 5C-E).

Antibodies A1, A2 and A3 appeared not optimal for detecting Aβ in Western blotting

We conducted further experiments to explore whether the new monoclonal Aβ antibodies were suitable for Western blotting. Frontal cortical lysates from the same cases used for immune-dot assays were processed for western blot analysis using antibodies A1, A2 and A3, as well as with the commercially available antibodies D12B2 and 6E10. Using 10% and 15% SDS-PAGE gels, the D12B2 antibody detected the peptide bands below the 10 kDa marker band, likely representing Aβ species in the AD samples with 10, 20 and 40 μg total protein loading. In contrast, this band was not detected in the lane loaded with the lysate (20 μg) from a control case (Fig. 6A, B). Molecular weight bands, e.g., ~20 kDa and 40 kDa, were also visible, presumably representing Aβ oligomers, as they were banded at ~100-130 kDa, which likely represent APP and its N-terminal fragments (Fig. 6A).

Using similar tissue extracting and immunoblotting protocols, antibodies 6E10 (Fig. 6C), A1 (Fig. 6D), A2 (Fig. 6E) and A3 (Fig. 6F) did not yield the expected Aβ bands in the AD human brain lysates as observed in the blotting with the D12B2 antibody. However, the signal of the internal loading control marker, GAPDH, was reblotted in the same membranes, with the band size/intensity appearing to be consistent with the amount of protein loading in the gel lanes (Fig. 6A-F).

Antibodies A1, A2 and A3 detected Aβ pathology in transgenic mouse models of AD

Transgenic mouse models play an essential role in the pathogenic investigation and drug discovery of AD. We then also explored the utility of the new monoclonal Aβ antibodies in detecting Aβ deposits in the brains of three commonly used transgenic model mice, using cryoprotected frozen sections from previous studies in our laboratory (Zhang et al., 2009; Cai et al., 2009; Zhou et al., 2018; Yan et al., 2012). Overall, these monoclonal antibodies exhibited high potency in visualizing Aβ deposits in the brains of all three transgenic mouse lines, including the APP/PS1, 5XFAD and 3XTg-AD mice. Thus, in parasagittal cerebral sections from an 18-month-old 3xTg-AD mouse, antibody A1 at 1:5000 dilution stained

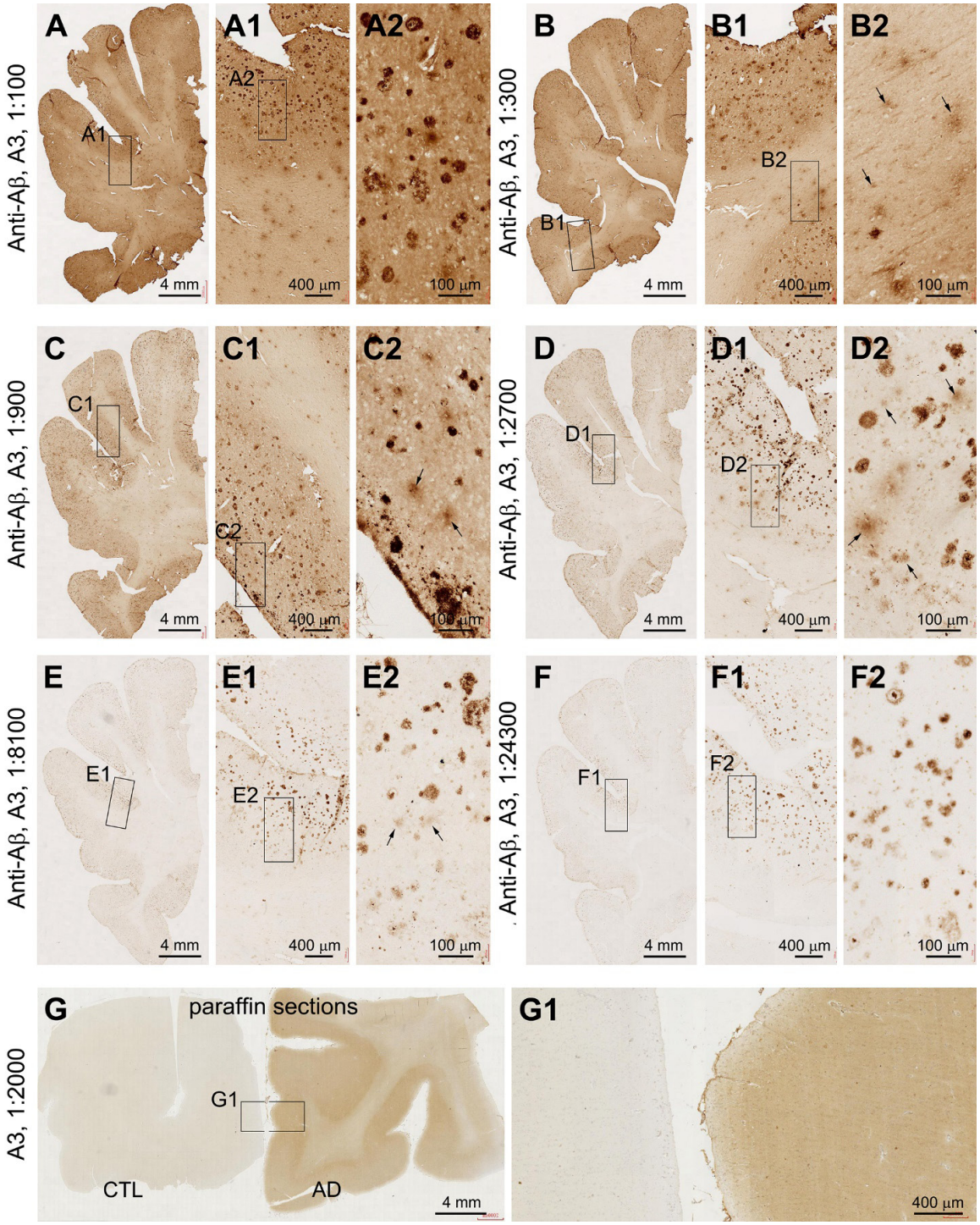

Figure 4. Immunolabeling of monoclonal antibody A3 in cryostat and paraffin sections from cases with and without AD-type neuropathology. Case information, antibody dilution, image orientation and scale bars are as indicated. The A3 antibody visualizes Aβ in frozen sections from an AD case **(A-F2)** at a range of dilutions. In paraffin sections, there is no labelling of Aβ in a section from an AD case, although the overall labeling intensity appears higher in the AD relative to control cases **(G-G1)**. Arrows show diffuse plaques in B2, C2, D2 and E2.

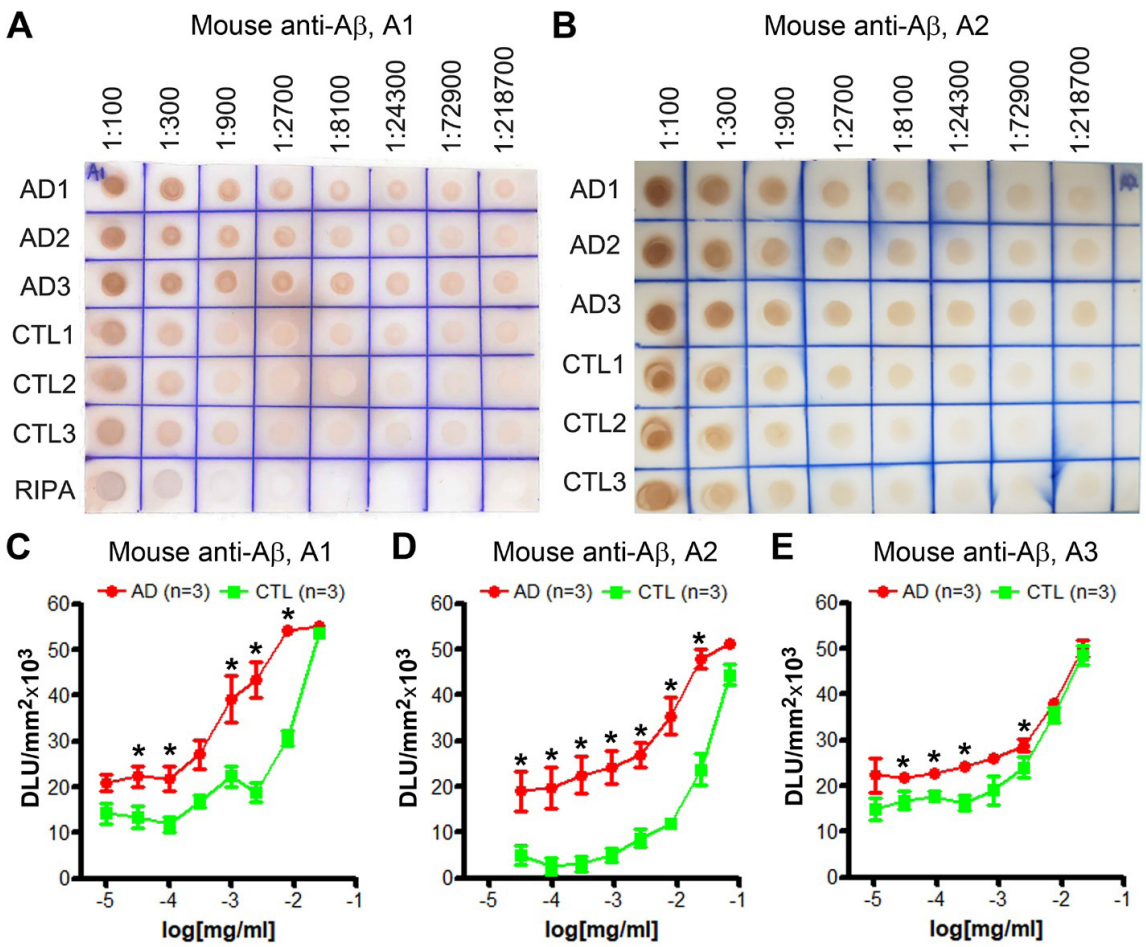

Figure 5. Immuno-dot blotting with monoclonal Aβ antibodies A1, A2 and A3. Panels **(A)** and **(B)** show representative images of the blotted membranes. Panels **(C-E)** show the densitometric data. *Statistically significant difference reached by student-t test.

a large amount of extracellular Aβ plaques in the hippocampal formation, especially in the subicular area (Fig. 7A, A1 and A2). There were also strongly labeled neuronal somata in layer V of the cerebral cortex and hippocampus (Figs. 7A1 and A2), which appeared to be largely pyramidal neurons based on their laminar location and morphology. The A2 antibody at 1:5000 showed Aβ deposition in the hippocampal formation (Fig. 7B, B1 and B2), whereas there was minor staining of neuronal soma in the cerebral cortex and hippocampus (Fig. 7B1 and B2). The A3 antibody at 1:5000 concentration detected extracellular plaques across the cerebral cortex in a coronal brain section from an 8-month-old APP/PS1 transgenic mouse, with lightly stained neuronal soma at high magnification (Fig. 7C, C1 and C2).

Discussion

Aβ antibodies are among the most widely used research tools in the biomedical field, given their extensive use in experimental studies and for the neuropathological diagnosis of AD. AD is one of the most significant challenges to human health and longevity worldwide in an era where population aging has attracted enormous jointed efforts in academia and industry to combat this devastating disease (Cui et al., 2020; Zhang et al., 2020; Guzman-Martinez et al., 2021; Scheltens et al., 2021; Lee et al., 2022; Tahami et al., 2022). In the present study, we evaluated 3 new monoclonal antibodies targeting Aβ. To our knowledge, this is the first study involving Aβ antibodies reportedly developed in China. We used post-mortem human

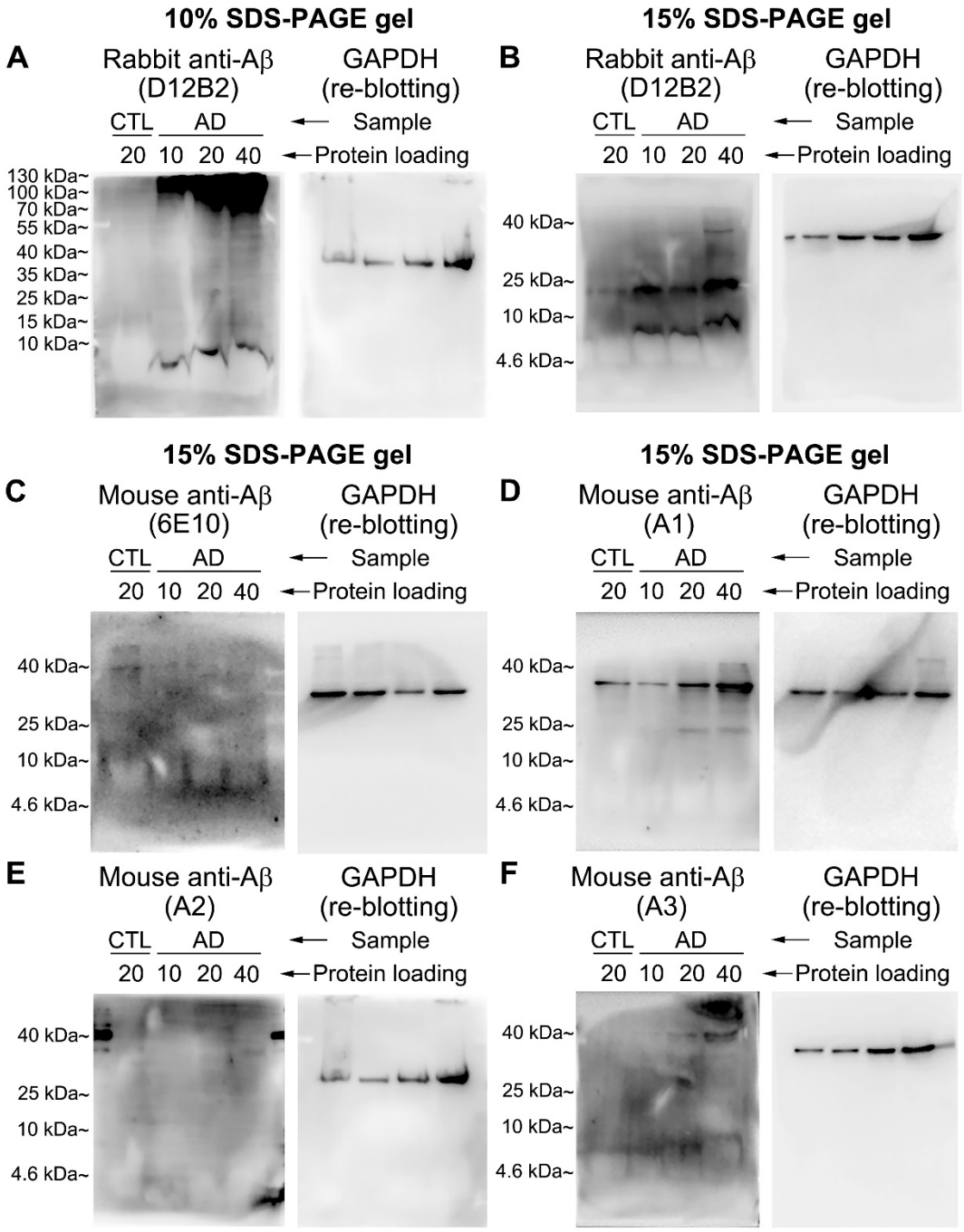

Figure 6. Representative images of Western blotting with monoclonal Aβ antibodies 6E10, D12B2, A1, A2 and A3. Panels **(A)** and **(B)** show that the putative Aβ bands <10 kDa molecular weight positions labeled with the commercial antibody D12B2 at 1:1000 dilution, with the signal in the AD samples being dose-dependent relatively to the amount of protein loading; the little signal is seen with the control (CTL) brain sample. The signal with antibody 6E10 (at 1:500) was not distinct **(C)**. The blotting signal at these molecular weight locations is either absent or fuzzy in the membranes processed with the monoclonal antibodies A1, A2 and A3 (at 1:1000) **(D-F)**.

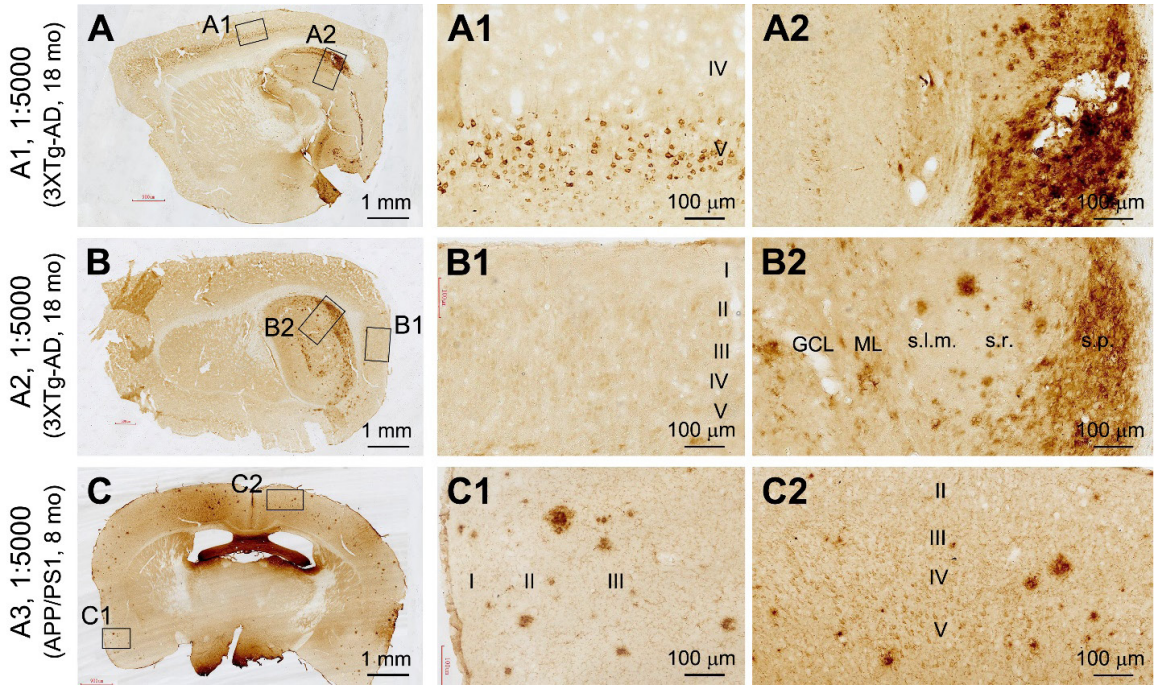

Figure 7. Representative images are showing immunolabeling by antibodies A1, A2 and A3 in brain sections from transgenic mice. Antibody dilutions, transgenic lines, animal ages and scale bars are marked on the left. Framed areas in the left low magnification images are enlarged as indicated. The three antibodies all visualized extracellular Aβ deposition primarily evident in the cerebral cortex and hippocampal formation. The Aβ pathology appears to be predominantly diffuse plaques in the 3xTg-AD mice **(A, A1, A2, B, B1 and B2)**, and can occur as compact plaques in the APP/PS1 mice (**C, C1 and C2)**. The A1 antibody also labels neuronal soma in the cerebral cortex and hippocampus **(A1, A2)**, whereas the A2 antibody exhibits little labeling in neuronal soma **(B1, B2)**. The A3 antibody labels compact-like extracellular plaques in the cerebral cortex with light reactivity of cellular profiles, likely pyramidal neurons **(C, C1 and C2)**.

brain tissue samples and performed assay controls to verify the specificity of each antibody, including the potency of these antibodies in detecting Aβ pathology in brain sections and Aβ levels in tissue lysates. In addition, we explored their potential use in experimental animal studies involving Aβ pathology in transgenic mouse models of AD.

Our immunohistochemical data indicated that the antibodies A1, A2 and A3 can specifically detect cerebral Aβ pathology in the human brain. Thus, all three antibodies were able to identify Aβ deposition in the cerebral cortex. This has been shown by the presence of compact and diffuse plaques in the parenchyma, along with CAA and meningeal/subpial amyloidosis. In contrast, no AB deposition was detected in the sections from the control samples. The pattern of Aβ deposition revealed by the three new antibodies (A1, A2 and A3) was comparable to that visualized by the commercial antibodies 6E10 and D12B2 and is also consistent with previously reported observations (Thal et al., 2002; Braak and Del Tredici, 2014; Cai et al., 2010; Hu et al., 2007; Tu et al., 2021). All three new antibodies seem well suited for Aβ immunohistochemistry for cryostat sections. However, antibody A3 does not appear suitable for paraffin sections for unknown reasons.

Given that the plaques are detectable at higher dilutions, antibodies A1, A2 and A3 seem very potent in immunolabeling Aβ pathology. High dilutions are preferred when using these antibodies. Otherwise, the background is high and can mask the specific labeling of plaques.

The results from the immune-dot blotting assays indicate that this set of new antibodies can detect an increase of Aβ levels in human brain lysates in a reasonably sensitive manner. Thus, the densities of Aβ products in cortical lysates of AD cases are consistently higher than in the lysates

of control cases, indicating the specificity of antibody reactivity to Aβ peptides. The difference in the levels of detected products between the two sample groups is significant when the working concentrations of the antibodies are very low diluted (i.e., in ng/ml concentration range). Therefore, these antibodies also appear potent in the immunobinding of Aβ products existing in soluble samples and, thus, could be optimized for measuring Aβ in biofluids. However, one pitfall of these antibodies is that our Western blotting experiments did not successfully reveal the particular Aβ species. In contrast, the positive assay control experiments using the D12B2 antibody detected the bands at 4-6 kDa consistent with Aβ peptides molecular weight. Therefore, these new monoclonal Aβ antibodies may not be suited for Western blotting under the conventional assay conditions applied in the current study.

Transgenic mouse models of AD exhibit the principal neuropathological hallmark of this disease and are widely used (Citron et al., 1992; Hsiao et al., 1996; Sasaguri et al., 2022). We showed that all the new monoclonal antibodies could detect the presence of Aβ pathology in the APP/PS1, 5XFAD and 3xTg-AD mouse models in the forms of compact and diffuse plaques. It should be noted that the antibody A1 also visualized layer V cortical and hippocampal pyramidal neurons. This intraneuronal labeling may relate to a cross-reaction to the mutant human APP overexpression in the transgenic animals, as denoted in previous studies (Zhang et al., 2009; Cai et al., 2010, 2012).

Data availability statement

The raw data supporting the conclusions of this article will be made available by the authors without undue reservation.

Ethics statement

Written consent for whole body donation for medical education and research was obtained from the donors or next of kin of subjects in compliance with the body/organ donation laws and regulations set by the Chinese government. The use of post-mortem human brains was approved by the Ethics Committee for Research and Education at Xiangya School of Medicine, in compliance with the Code of Ethics of the World Medical Association (Declaration of Helsinki).

Author contributions

All authors read and approved the final manuscript. Conceptualization: HYC, CC, XXY; Methodology: HYC, JA, CY, XLC, JJ, TT, ET; Data analysis: JJ, CY, TT, QLZ; Writing - original draft preparation: HYC, JA, XXY; Writing - review and editing: CC, XXY; Funding acquisition: ET, XXY; Resources: CC.

Funding

This study was by the National Natural Science Foundation of China (grant #91632116), Ministry of Science and Technology of China (#2021ZD0201103 and #2021ZD0201803), Hunan Provincial Science & Technology Foundation (grant #2018JJ2552), and Jilin Provincial Science and Technology Department (#YDZJ202201ZYTS186).

Acknowledgments

We thank Xiao-Hua Tang for help with Motic light microscopic imaging and Dan-Dan Hu, Qiang Li, Qian-Li Shen for human brain banking.

Competing interests

GeneScience Pharmaceuticals Co., Ltd employs Author Chong Che. The remaining authors declare that the research was conducted without any commercial or financial relationships construed as a potential conflict of interest.

References

Alawode DOT, Heslegrave AJ, Ashton NJ, Karikari TK, Simrén J, Montoliu-Gaya L, Pannee J, O Connor A, Weston PSJ, Lantero-Rodriguez J, Keshavan A, Snellman A, Gobom J, Paterson RW, Schott JM, Blennow K, Fox NC, Zetterberg H. Transitioning from cerebrospinal fluid to blood tests to facilitate diagnosis and disease monitoring in Alzheimer's disease. J Intern Med. 2021; 290(3):583-601.

Alonso Adel C, ElAkkad E, Gong C, Liu F, Tanaka T, Kudo T, Tatebayashi Y, Pei J, Wang J, Khatoon S, Flory M, Ghetti B, Gozes I, Novak M, Novak M, Robakis NK, de Leon M, Iqbal M. Inge Grundke-Iqbal, Ph.D. (1937–2012): the discoverer of the abnormal hyperphosphorylation of tau

in Alzheimer's disease. J Mol Neurosci. 2013; 49(2):430-5.

Beach TG. A History of Senile Plaques: From Alzheimer to Amyloid Imaging. J Neuropathol Exp Neurol. 2022; 81(6):387-413.

Braak H, Braak E. Demonstration of amyloid deposits and neurofibrillary changes in whole brain sections. Brain Pathol. 1991; 1(3):213-6.

Braak H, Del Tredici K. Are cases with tau pathology occurring in the absence of Aβ deposits part of the AD-related pathological process? Acta Neuropathol. 2014; 128(6):767-72.

Cai Y, Xiong K, Zhang XM, Cai H, Luo XG, Feng JC, Clough RW, Struble RG, Patrylo PR, Chu Y, Kordower JH, Yan XX. β-Secretase-1 elevation in aged monkey and Alzheimer's disease human cerebral cortex occurs around the vasculature in partnership with multisystem axon terminal pathogenesis and β-amyloid accumulation. Eur J Neurosci. 2010; 32(7):1223-38.

Cai Y, Zhang XM, Macklin LN, Cai H, Luo XG, Oddo S, Laferla FM, Struble RG, Rose GM, Patrylo PR, Yan XX. BACE1 elevation is involved in amyloid plaque development in the triple transgenic model of Alzheimer's disease: differential Aβ antibody labeling of early-onset axon terminal pathology. Neurotox Res. 2012; 21(2):160-74.

Caselli RJ, Beach TG, Knopman DS, Graff-Radford NR. Alzheimer Disease: Scientific Breakthroughs and Translational Challenges. Mayo Clin Proc. 2017; 92(6):978-994.

Checler F, Afram E, Pardossi-Piquard R, Lauritzen I. Is γ-secretase a beneficial inactivating enzyme of the toxic APP C-terminal fragment C99? J Biol Chem. 2021; 296:100489.

Cho Y, Bae HG, Okun E, Arumugam TV, Jo DG. Physiology and pharmacology of amyloid precursor protein. Pharmacol Ther. 2022; 235:108122.

Citron M, Westaway D, Xia W, Carlson G, Diehl T, Levesque G, Johnson-Wood K, Lee M, Seubert P, Davis A, Kholodenko D, Motter R, Sherrington R, Perry B, Yao H, Strome R, Lieberburg I, Rommens J, Kim S, Schenk D, Fraser P, St George Hyslop P, Selkoe DJ. Mutant presenilins of Alzheimer's disease increase production of 42-residue amyloid beta-protein in both transfected cells and transgenic mice. Nat Med. 1997; 3(1):67-72.

Cong C, Zhang W, Qian X, Qiu W, Ma C. Significant Overlap of α-Synuclein, Amyloid-β, and Phospho-Tau Pathologies in Neuropathological Diagnosis of Lewy-related Pathology: Evidence from China Human Brain Bank. J Alzheimers Dis. 2021; 80(1):447-458.

Critchley M. Critical Review: THE NATURE AND SIGNIFICANCE OF SENILE PLAQUES. J Neurol Psychopathol. 1929; 10(38):124-39.

Cui L, Hou NN, Wu HM, Zuo X, Lian YZ, Zhang CN, Wang ZF, Zhang X, Zhu JH. Prevalence of Alzheimer's Disease and Parkinson's Disease in China: An Updated Systematical Analysis. Front Aging Neurosci. 2020;12:603854

Gao Y, Liu J, Wang J, Liu Y, Zeng LH, Ge W, Ma C. Proteomic analysis of human hippocampal subfields provides new insights into the pathogenesis of Alzheimer's disease and the role of glial cells. Brain Pathol. 2022; 32(4):e13047.

García-Marín V, García-López P, Freire M. Cajal's contributions to the study of Alzheimer's disease. J Alzheimers Dis. 2007; 12(2):161-74.

Glenner GG, Wong CW. Alzheimer's disease: initial report of the purification and characterization of a novel cerebrovascular amyloid protein. Biochem Biophys Res Commun. 1984; 120(3):885-90.

Goedert M, Wischik CM, Crowther RA, Walker JE, Klug A. Cloning and sequencing of the cDNA encoding a core protein of the paired helical filament of Alzheimer disease: identification as the microtubule-associated protein tau. Proc Natl Acad Sci U S A. 1988; 85(11):4051-5.

Griffith CM, Xie MX, Qiu WY, Sharp AA, Ma C, Pan A, Yan XX, Patrylo PR. Aberrant expression of the pore-forming KATP channel subunit Kir6. 2 in hippocampal reactive astrocytes in the 3XTg-AD mouse model and human Alzheimer's disease. Neuroscience 2016; 336: 81-101.

Grundke-Iqbal I, Iqbal K, Tung YC, Quinlan M, Wisniewski HM, Binder LI. Abnormal phosphorylation of the microtubule-associated protein tau (tau) in Alzheimer

cytoskeletal pathology. Proc Natl Acad Sci U S A. 1986; 83(13):4913-7.

Guzman-Martinez L, Calfío C, Farias GA, Vilches C, Prieto R, Maccioni RB. New Frontiers in the Prevention, Diagnosis, and Treatment of Alzheimer's Disease. J Alzheimers Dis. 2021; 82(s1):S51-S63.

Guzman-Martinez L, Maccioni RB, Farías GA, Fuentes P, Navarrete LP. Biomarkers for Alzheimer's Disease. Curr Alzheimer Res. 2019; 16(6):518-528.

Hampel H, Vassar R, De Strooper B, Hardy J, Willem M, Singh N, Zhou J, Yan R, Vanmechelen E, De Vos A, Nisticò R, Corbo M, Imbimbo BP, Streffer J, Voytyuk I, Timmers M, Tahami Monfared AA, Irizarry M, Albala B, Koyama A, Watanabe N, Kimura T, Yarenis L, Lista S, Kramer L, Vergallo A. The β-Secretase BACE1 in Alzheimer's Disease. Biol Psychiatry. 2021; 89(8):745-756.

Hsiao K, Chapman P, Nilsen S, Eckman C, Harigaya Y, Younkin S, Yang F, Cole G Correlative memory deficits, Abeta elevation, and amyloid plaques in transgenic mice. Science. 1996; 274(5284):99-102.

Hu X, Hu ZL, Li Z, Ruan CS, Qiu WY, Pan A, Li CQ, Cai Y, Shen L, Chu Y, Tang BS, Cai H, Zhou XF, Ma C, Yan XX. Sortilin Fragments Deposit at Senile Plaques in Human Cerebrum. Front Neuroanat. 2017; 11:45.

Hur JY. γ-Secretase in Alzheimer's disease. Exp Mol Med. 2022; 54(4):433-446.

Jeremic D, Jiménez-Díaz L, Navarro-López JD. Past, present and future of therapeutic strategies against amyloid-β peptides in Alzheimer's disease: a systematic review. Ageing Res Rev. 2021; 72:101496.

Jia Y, Wang X, Chen Y, Qiu W, Ge W, Ma C. Proteomic and Transcriptomic Analyses Reveal Pathological Changes in the Entorhinal Cortex Region that Correlate Well with Dysregulation of Ion Transport in Patients with Alzheimer's Disease. Mol Neurobiol. 2021; 58(8):4007-4027.

Jiang J, Yang C, Ai JQ, Zhang QL, Cai XL, Tu T, Wan L, Wang XS, Wang H, Pan A, Manavis J, Gai WP, Che C, Tu E, Wang XP, Li ZY, Yan XX. Intraneuronal sortilin aggregation relative to granulovacuolar degeneration, tau pathogenesis and sorfra plaque formation in human hippocampal formation. Front. Aging Neurosci. 2022; 14: 926904

Khurshid B, Rehman AU, Muhammad S, Wadood A, Anwar J. Toward the Noninvasive Diagnosis of Alzheimer's Disease: Molecular Basis for the Specificity of Curcumin for Fibrillar Amyloid-β. ACS Omega. 2022; 7(25):22032-22038.

Lee J, Howard RS, Schneider LS. The Current Landscape of Prevention Trials in Dementia. Neurotherapeutics. 2022; 19(1):228-247.

Liu P, Yang Q, Yu N, Cao Y, Wang X, Wang Z, Qiu WY, Ma C. Phenylalanine Metabolism Is Dysregulated in Human Hippocampus with Alzheimer's Disease Related Pathological Changes. J Alzheimers Dis. 2021; 83(2):609-622.

Ma C, Bao AM, Yan XX, Swaab DF. Progress in Human Brain Banking in China. Neurosci Bull. 2019; 35(2):179-182.

Macklin L, Griffith CM, Cai Y, Rose GM, Yan XX, Patrylo PR. Glucose tolerance and insulin sensitivity are impaired in APP/PS1 transgenic mice prior to amyloid plaque pathogenesis and cognitive decline. Exp Gerontol. 2016; 88: 9-18

Masters CL, Simms G, Weinman NA, Multhaup G, McDonald BL, Beyreuther K. Amyloid plaque core protein in Alzheimer disease and Down syndrome. Proc Natl Acad Sci U S A. 1985; 82(12):4245-9.

Novak M, Wischik CM, Edwards P, Pannell R, Milstein C. Characterisation of the first monoclonal antibody against the pronase resistant core of the Alzheimer PHF. Prog Clin Biol Res. 1989; 317:755-61.

Ohry A, Buda O. Teofil Simchowicz (1879-1957): the scientist who coined senile plaques in neuropathology. Rom J Morphol Embryol. 2015; 56(4):1545-8.

Oĭfa AI. Paul Divry--founder of the concept of cerebral amyloidosis. Zh Nevropatol Psikhiatr Im S S Korsakova. 1973;73(7):1078-82.

Patel S, Bansoad AV, Singh R, Khatik GL. BACE1: A Key Regulator in Alzheimer's Disease Progression and Current Development of its Inhibitors. Curr Neuropharmacol. 2022; 20(6):1174-1193.

Qiu W, Zhang H, Bao A, Zhu K, Huang Y, Yan X, Zhang J, Zhong C, Shen Y, Zhou J, Zheng X, Zhang L, Shu Y, Tang B, Zhang Z, Wang G,

Zhou R, Sun B, Gong C, Duan S, Ma C. Standardized Operational Protocol for Human Brain Banking in China. Neurosci Bull. 2019; 35(2):270-276.

Sasaguri H, Hashimoto S, Watamura N, Sato K, Takamura R, Nagata K, Tsubuki S, Ohshima T, Yoshiki A, Sato K, Kumita W, Sasaki E, Kitazume S, Nilsson P, Winblad B, Saito T, Iwata N, Saido TC. Recent Advances in the Modeling of Alzheimer's Disease. Front Neurosci. 2022; 16:807473.

Scheltens P, De Strooper B, Kivipelto M, Holstege H, Chételat G, Teunissen CE, Cummings J, van der Flier WM. Alzheimer's disease. Lancet. 2021; 397(10284):1577-1590.

Serrano-Pozo A, Frosch MP, Masliah E, Hyman BT. Neuropathological alterations in Alzheimer disease. Cold Spring Harb Perspect Med. 2011;1(1): a006189.

Shi YB, Tu T, Jiang J, Zhang QL, Ai JQ, Pan A, Manavis J, Tu E, Yan XX. Early Dendritic Dystrophy in Human Brains with Primary Age-Related Tauopathy. Front Aging Neurosci. 2020; 12:596894.

Tahami Monfared AA, Byrnes MJ, White LA, Zhang Q. Alzheimer's Disease: Epidemiology and Clinical Progression. Neurol Ther. 2022; 11(2):553-569.

Tang K, Wan M, Zhang H, Zhang Q, Yang Q, Chen K, Wang N, Zhang D, Qiu W, Ma C. The top 100 most-cited articles citing human brain banking from 1970 to 2020: a bibliometric analysis. Cell Tissue Bank. 2020; 21(4):685-697.

Thal DR, Rüb U, Orantes M, Braak H. Phases of A beta-deposition in the human brain and its relevance for the development of AD. Neurology. 2002; 58(12):1791-800.

Tu T, Jiang J, Zhang QL, Wan L, Li YN, Pan A, Manavis J, Yan XX. Extracellular Sortilin Proteopathy Relative to β-Amyloid and Tau in Aged and Alzheimer's Disease Human Brains. Front Aging Neurosci. 2020; 12:93.

Wischik CM, Novak M, Thøgersen HC, Edwards PC, Runswick MJ, Jakes R, Walker JE, Milstein C, Roth M, Klug A. Isolation of a fragment of tau derived from the core of the paired helical filament of Alzheimer disease. Proc Natl Acad Sci U S A. 1988; 85(12):4506-10.

Xiong F, Ge W, Ma C. Quantitative proteomics reveals distinct composition of amyloid plaques in Alzheimer's disease. Alzheimers Dement. 2019; 15(3):429-440.

Xu B, Gao Y, Zhan S, Xiong F, Qiu W, Qian X, Wang T, Wang N, Zhang D, Yang Q, Wang R, Bao X, Dou W, Tian R, Meng S, Gai WP, Huang Y, Yan XX, Ge W, Ma C. Quantitative protein profiling of hippocampus during human aging. Neurobiol Aging. 2016; 39:46-56.

Yan XX, Xiong K, Luo XG, Struble RG, Clough RW. beta-Secretase expression in normal and functionally deprived rat olfactory bulbs: inverse correlation with oxidative metabolic activity. J Comp Neurol. 2007; 501(1):52-69.

Yan XX, Cai Y, Shelton J, Deng SH, Luo XG, Oddo S, Laferla FM, Cai H, Rose GM, Patrylo PR. Chronic temporal lobe epilepsy is associated with enhanced Alzheimer-like neuropathology in 3×Tg-AD mice. PLoS One. 2012;7(11):e48782.

Yan XX, Ma C, Bao AM, Wang XM, Gai WP. Brain banking as a cornerstone of neuroscience in China. Lancet Neurol. 2015; 14(2):136.

Yang W, Guo X, Tu Z, Chen X, Han R, Liu Y, Yan S, Wang Q, Wang Z, Zhao X, Zhang Y, Xiong X, Yang H, Yin P, Wan H, Chen X, Guo J, Yan XX, Liao L, Li S, Li XJ. PINK1 kinase dysfunction triggers neurodegeneration in the primate brain without impacting mitochondrial homeostasis. Protein Cell. 2022; 13(1):26-46.

Zhang L, Jiang Y, Zhu J, Liang H, He X, Qian J, Lin H, Tao Y, Zhu K. Quantitative Assessment of Hippocampal Tau Pathology in AD and PART. J Mol Neurosci. 2020; 70(11):1808-1811.

Zhang X, Sun B, Wang X, Lu H, Shao F, Rozemuller AJM, Liang H, Liu C, Chen J, Huang M, Zhu K. Phosphorylated TDP-43 Staging of Primary Age-Related Tauopathy. Neurosci Bull. 2019; 35(2):183-192.

Zhang XM, Cai Y, Xiong K, Cai H, Luo XG, Feng JC, Clough RW, Struble RG, Patrylo PR, Yan XX. Beta-secretase-1 elevation in transgenic mouse models of Alzheimer's disease is associated with synaptic/axonal pathology and amyloidogenesis: implications for neuritic plaque development. Eur J Neurosci. 2009; 30(12):2271-83.

Zhang Y, Li Y, Ma L. Recent advances in research on Alzheimer's disease in China. J Clin Neurosci. 2020; 81:43-46.

Zhao J, Fu Y, Yasvoina M, Shao P, Hitt B, O'Connor T, Logan S, Maus E, Citron M, Berry R, Binder L, Vassar R. Beta-site amyloid precursor protein cleaving enzyme 1 levels become elevated in neurons around amyloid plaques: implications for Alzheimer's disease pathogenesis. J Neurosci. 2007; 27(14):3639-49.

Zhou FQ, Jiang J, Griffith CM, Patrylo PR, Cai H, Chu Y, Yan XX. Lack of human-like extracellular sortilin neuropathology in transgenic Alzheimer's disease model mice and macaques. Alzheimers Res Ther. 2018; 10(1):40.

Zhu K, Wang X, Sun B, Wu J, Lu H, Zhang X, Liang H, Zhang D, Liu C. Primary Age-Related Tauopathy in Human Subcortical Nuclei. Front Neurosci. 2019; 13:529.